

Light vector mediators at direct detection experiments

Valentina De Romeri,^{1, a} Dimitrios K. Papoulias,^{2, b} and Christoph A. Ternes^{3, c}

¹*Instituto de Física Corpuscular (CSIC-Universitat de València),*

Parc Científic UV C/ Catedrático José Beltrán, 2 E-46980 Paterna (Valencia) - Spain

²*Department of Physics, National and Kapodistrian University of Athens,*

Zografou Campus GR-15772 Athens, Greece

³*Istituto Nazionale di Fisica Nucleare (INFN),*

Laboratori Nazionali del Gran Sasso, 67100 Assergi, L'Aquila (AQ), Italy

Solar neutrinos induce elastic neutrino-electron scattering in dark matter direct detection experiments, resulting in detectable event rates at current facilities. We analyze recent data from the XENONnT, LUX-ZEPLIN, and PandaX-4T experiments and we derive stringent constraints on several $U(1)'$ extensions of the Standard Model, accommodating new neutrino-electron interactions. We provide bounds on the relevant coupling and mass of light vector mediators for a variety of models, including the anomaly-free $B - L$ model, lepton flavor-dependent interactions like $L_\alpha - L_\beta$, $B - 2L_e - L_{\mu,\tau}$, $B - 3L_\alpha$, and $B + 2L_\mu + 2L_\tau$ models. We compare our results with other limits obtained in the literature from both terrestrial and astrophysical experiments. Finally, we present forecasts for improving current bounds with a future experiment like DARWIN.

Keywords: light mediators, dark matter detectors, neutrinos

CONTENTS

I. Introduction	2
II. Theoretical framework	4
A. $E\nu$ ES in the Standard Model	4
B. $E\nu$ ES in models with an extra $U(1)'$ symmetry	4
III. Data analysis	5
A. Current experiments	6
B. DARWIN sensitivity	7
IV. Results	7
The $B - L$ model	8
The $B - 2L_e - L_{\mu/\tau}$ models	10
The $B - 3L_\alpha$ models	10
The $L_\alpha - L_\beta$ models	10
The $L_e + 2L_\mu + 2L_\tau$ model	12
V. Conclusions	12
Acknowledgments	12
References	14

^a deromeri@ific.uv.es

^b dkapoulias@phys.uoa.gr

^c christoph.ternes@lngs.infn.it

I. INTRODUCTION

Dark Matter (DM) Direct Detection (DD) experiments [1, 2], although primarily designed for DM searches, have been recently recognized as favorable facilities to probe new physics beyond the weakly interacting massive particles (WIMPs) paradigm [3]. Indeed, and despite the so far eluding WIMP detection, the latest generation of DM DD experiments — including low-threshold ($E_{\text{thr}} = 1$ keV) dual-phase liquid xenon (LXe) detectors developed by the XENON (Italy) [4–6], LUX-ZEPLIN (LZ) in the USA [7–9], and PandaX (China) [10–12] collaborations — have reached world-leading sensitivities also on alternative physics beyond the SM (BSM), for instance boosted-DM scenarios [13, 14], dark photons [15], axion-like particles [16], novel hidden sectors [17], fermionic absorption DM [18] and gravitational waves [19]. The physics program of DD facilities will continue and intensify with next-generation detectors [3, 20, 21] such as those planned by the DARWIN Collaboration [22] that aspire to achieve very low sensitivities leveraging its multi-ton exposure, low background and low threshold. Towards this purpose the XLZD Consortium (XENON, LZ, DARWIN) aims to develop a 60-ton LXe detector in the next decade [23] that will probe WIMPs down to the neutrino fog. At the same time, further advances based on liquid argon (LAr) technology are currently under development by the Global Argon Dark Matter Collaboration (GADMC) [24], with near-term activities focusing on the construction of the DarkSide-20k detector at Laboratori Nazionali del Gran Sasso (LNGS), and the ultimate goal being the construction of a 300-ton argon detector.

At present, the large fiducial volumes of LXe detectors available at the XENONnT (5.9 ton), LZ (5.5 ton) and PandaX-4T (3.7 ton) experiments have already allowed the collaborations to accumulate exposures of 1.16, 0.90, and 0.63 ton \times year, respectively, in a rather short amount of data-collection time during their first run. This, together with their extremely low-threshold capabilities¹ has prompted an impressive flourishing of theoretical activity in the search for new physics, inspiring an exhaustive number of phenomenological analyses.

Strikingly, the increase in target size and sensitivity of current DD detectors has opened a whole new window for the observation of the scattering of solar neutrinos. While constituting an irreducible background for DM searches, through the so-called ν -floor [25] or fog [26], sizable fluxes of solar neutrinos also provide new opportunities for probing neutrino properties [27–29] and new physics connected to the neutrino sector [30–37].

Neutrinos coming from the Sun can induce elastic neutrino-electron scattering ($E\nu$ ES) and coherent elastic neutrino-nucleus scattering ($CE\nu$ NS) events in DM DD experiments, both having a strong degeneracy with the corresponding DM-electron [33, 38] and DM-nucleus signals [39]. Given the current detector technology, for $E\nu$ ES ($CE\nu$ NS) only the pp and ${}^7\text{Be}$ (${}^8\text{B}$) components of the total solar neutrino flux contribute significantly to the detectable event rates. However, since the $CE\nu$ NS rate is suppressed at current detectors due to threshold limitations, solar neutrinos at DM DD experiments are currently detected mainly through $E\nu$ ES.

In this work we are interested in determining the potential of current DM DD experiments, namely XENONnT, LZ and PandaX-4T in probing new physics in the neutrino sector through $E\nu$ ES induced by solar neutrinos. Analyses along this line have been done previously to investigate neutrino properties and BSM interactions. These include, for instance, neutrino electromagnetic properties such as effective [27, 29] and fundamental [40] neutrino magnetic moments. Future data from e.g. a DARWIN-type experiment will allow for precision searches of electroweak and oscillation parameters as detailed in Ref. [22], while the possibility of probing flavor-dependent radiative corrections to $CE\nu$ NS has been explored in Ref. [41]. Neutrino nonstandard interactions (NSI) have been addressed in Ref. [42] using existing data (XENONnT and LZ) and providing

¹ Note that the energy threshold is different depending on the detector materials. In the case of liquid xenon, it is around $E_{\text{thr}} \sim 1$ keV.

forecasts for DARWIN, complementing the NSI landscape probed by CE ν NS experiments and oscillation searches.

Going one step beyond effective NSI, our goal is to explore new neutrino interactions mediated by light vector bosons, that can arise in several motivated $U(1)'$ [43] extensions of the SM. We will focus on light vector mediators, that are expected to generate spectral distortions, through an increase of the E ν ES differential cross section, for sufficiently small mediator masses and low recoil energies. DM DD experiments, characterised by low-energy thresholds, are suitable facilities to probe such spectral features [15, 44, 45]. Note that in the limit of effective interactions, or equivalently, heavy mediators (with masses much larger than the typical momentum transfer of the process) the NSI formalism used in Ref. [42] can be directly related to the $U(1)'$ models that we will consider, see, e.g., Ref. [46].

We will focus on several BSM models with an extended gauge sector, namely an additional $U(1)'$ symmetry. These will include: the anomaly-free $B - L$ model [43, 47, 48], B being the baryon number and L the total lepton number; lepton flavor-dependent interactions like the $L_e - L_\mu$, $L_\mu - L_\tau$ and $L_e - L_\tau$ [49–52] $U(1)'$ models, also free of quantum anomalies; the $B - 2L_e - L_\mu$ and $B - 2L_e - L_\tau$ models [53, 54], where leptons have generation-dependent charges under the $U(1)'$ symmetry; the $B - 3L_e$ [46, 53–57], $B - 3L_\mu$ and $B - 3L_\tau$ scenarios [46, 53, 56–62] and $L_e + 2L_\mu + 2L_\tau$ [46].

There is a number of previous works involving light-mediator analyses of DM DD data: Ref. [40] analyzed general light mediators exploiting recent data from the LZ [9] and XENONnT [6] experiments, while Ref. [63] performed a similar study employing recent data by the PandaX-II [64] experiment. Reference [65] set constraints on general neutrino interactions using SENSEI, Edelweiss, and SuperCDMS data and as well as projections for future experiments. These studies complement bounds inferred using CE ν NS data by COHERENT [66] and E ν ES data at Borexino [67], as well as forecasts for the DUNE near detector [68] and FASER [69]. Additional studies have focused on anomaly-free $U(1)'$ models. For instance, Ref. [70] explored the implications of XENONnT and Borexino E ν ES data on the $B - L$ model, while Refs. [34, 36] focused on projections for the $L_\mu - L_\tau$ model at DARWIN. More recently, Ref. [71] explored general light mediators as well as $B - L$ and $L_\mu - L_\tau$ gauge symmetries via both CE ν NS and E ν ES at next generation DM DD experiments. Solar neutrino constraints on light mediators have been set by looking at CE ν NS data from CDEX-10 in Ref. [72].

Our work adds to these previous studies by means of a detailed analysis of several motivated $U(1)'$ scenarios based on the most recent data from the XENONnT [6], LZ [9], and PandaX-4T [11] experiments and by providing sensitivities expected at a future DARWIN-like facility. Moreover, our present analysis improves upon previous E ν ES-based work on light mediators [40] as described in the following. First, we use real, recent data from the current most sensitive experiments. Besides providing separate bounds for each of them, we also present for the first time a combined analysis. Secondly, we carry out an improved statistical analysis by treating the background components of LZ, XENONnT and PandaX-4T separately, together with their own uncertainty, closely following Ref. [29]. Finally, we perform a comprehensive exploration of various vector mediators that go beyond the simplest $B - L$ model, as already introduced. Our work is aimed at extending and complementing the results obtained in Ref. [54], that addresses bounds on several types of $U(1)'$ models using recent COHERENT data.

The remainder of the work is organized as follows: in Section II we discuss the effect of additional $U(1)'$ symmetries on the E ν ES process. In Section III we detail the analysis procedure for current (III A) and future (III B) DM DD experiments. In Section IV we present the results of our analyses and compare with other bounds from the literature before closing in Section V.

II. THEORETICAL FRAMEWORK

We are interested in determining the potential of current DM DD experiments, to probe new light vector bosons through $E\nu$ ES induced by solar neutrinos on atomic electrons in the detectors' targets. In this section we introduce the $E\nu$ ES process, and provide its cross section both within the SM and in the framework of BSM extensions with an additional $U(1)'$ symmetry.

A. $E\nu$ ES in the Standard Model

In the SM, the differential $E\nu$ ES cross section, with respect to the electron recoil energy T_e , is given by

$$\left. \frac{d\sigma_{\nu\alpha\mathcal{A}}}{dT_e} \right|^{SM} = Z_{\text{eff}}^{\mathcal{A}}(T_e) \frac{G_F^2 m_e}{2\pi} \left[(g_V + g_A)^2 + (g_V - g_A)^2 \left(1 - \frac{T_e}{E_\nu}\right)^2 - (g_V^2 - g_A^2) \frac{m_e T_e}{E_\nu^2} \right], \quad (1)$$

where G_F , E_ν and m_e denote the Fermi constant, the incoming neutrino energy and the electron mass, respectively. The SM vector and axial-vector couplings depend on the flavor α of the incoming neutrino ν_α and read $g_V = 2 \sin^2 \theta_W - 1/2 + \delta_{\alpha e}$, $g_A = -1/2 + \delta_{\alpha e}$, $\sin^2 \theta_W = 0.23857$ being the weak mixing angle in the low-energy regime. The term $\delta_{\alpha e}$ is due to the fact that in the case of incoming electron neutrinos both neutral and charged currents are relevant, while for the case of ν_μ and ν_τ $E\nu$ ES acquires contributions from neutral currents only. Assuming that the target electrons are bound in the atomic nuclei \mathcal{A} of the detector material, the factor $Z_{\text{eff}}^{\mathcal{A}}(T_e)$ in Eq. (1) accounts for the effective number of electrons that can be ionized given an energy dissipation T_e , and it is taken from the Hartree-Fock calculations provided in Ref. [73].

B. $E\nu$ ES in models with an extra $U(1)'$ symmetry

Within the context of a general $U(1)'$ symmetry, with a new vector mediator Z' with mass $m_{Z'}$, the Lagrangian describing neutrino-fermion interactions reads

$$\mathcal{L}_{Z'} = g_{Z'} Z'_\mu \left(Q_{Z'}^f \bar{f} \gamma^\mu f + \sum_\alpha Q_{Z'}^{\nu_\alpha} \bar{\nu}_{\alpha,L} \gamma^\mu \nu_{\alpha,L} \right) + \frac{1}{2} m_{Z'}^2 Z'^\mu Z'_\mu, \quad (2)$$

where for the case of $E\nu$ ES $f = e$, $g_{Z'}$ is the new coupling while $Q_{Z'}^i$ denote the individual vector charges (see Tab. I). Then, for incoming neutrinos of flavor α , the new contribution to $E\nu$ ES can be obtained from the SM expression of the cross section given in Eq. (1) by changing

$$g_V \rightarrow g_V^{\text{SM}} + \frac{(g_{Z'})^2 Q_{Z'}^e Q_{Z'}^{\nu_\alpha}}{\sqrt{2} G_F (2m_e T_e + m_{Z'}^2)}. \quad (3)$$

The above expression is valid in both low- and high-mass regimes, noting that the typical momentum transfer involved in DM DD experiments is $|\mathbf{q}| \approx \sqrt{2m_e T_e} \sim \mathcal{O}(100)$ keV.

In this paper we consider the following models: $B - L$, $B - 3L_\alpha$, $B - 2L_e - L_{\mu,\tau}$, $L_\alpha - L_\beta$ and $L_e + 2L_\mu + 2L_\tau$ with the corresponding charges summarized in Tab. I. For completeness, let us stress that unlike the $B - L$ case where all neutrino fluxes contribute equally to new physics cross sections, in lepton flavor-dependent models the new physics contributions come only from the corresponding flavor component of the total solar neutrino flux, weighted through the charges given in Tab. I.

Model	$Q_{Z'}^u$	$Q_{Z'}^d$	$Q_{Z'}^{e/\nu_e}$	$Q_{Z'}^{\mu/\nu_\mu}$	$Q_{Z'}^{\tau/\nu_\tau}$
$B - L$	1/3	1/3	-1	-1	-1
$B - 3L_e$	1/3	1/3	-3	0	0
$B - 3L_\mu$	1/3	1/3	0	-3	0
$B - 3L_\tau$	1/3	1/3	0	0	-3
$B - 2L_e - L_\mu$	1/3	1/3	-2	-1	0
$B - 2L_e - L_\tau$	1/3	1/3	-2	0	-1
$L_e - L_\mu$	0	0	1	-1	0
$L_e - L_\tau$	0	0	1	0	-1
$L_\mu - L_\tau$	0	0	0	1	-1
$L_e + 2L_\mu + 2L_\tau$	0	0	1	2	2

TABLE I: Individual charges in the $U(1)'$ models considered in this work.

On the other hand, in the case of the leptophilic model $L_\mu - L_\tau$, since there is no direct coupling to electrons, the new contribution arises at the one-loop level [54]²:

$$g_V \rightarrow g_V^{\text{SM}} - \frac{\sqrt{2}\alpha_{\text{em}}g_{Z'}^2(\delta_{\alpha\mu} - \delta_{\alpha\tau})}{\pi G_F(2m_e T_e + m_V^2)} \epsilon_{\tau\mu}(|\vec{q}|), \quad (4)$$

where α_{em} is the fine-structure constant while the couplings $\epsilon_{\tau\mu}$ can be approximated as

$$\epsilon_{\tau\mu}(|\vec{q}|) = \int_0^1 x(1-x) \ln \left(\frac{m_\tau^2 + x(1-x)|\vec{q}|^2}{m_\mu^2 + x(1-x)|\vec{q}|^2} \right) dx \approx \frac{1}{6} \ln \left(\frac{m_\tau^2}{m_\mu^2} \right). \quad (5)$$

Similarly, in the framework of the $B - 3L_{\mu,\tau}$ models the corresponding $\text{E}\nu\text{ES}$ contribution also arises at the one-loop level and reads

$$g_V \rightarrow g_V^{\text{SM}} - \frac{\sqrt{2}\alpha_{\text{em}}g_{Z'}^2 Q_{Z'}^\alpha \delta_{\alpha(\mu/\tau)}}{\pi G_F(2m_e T_e + m_V^2)} \tilde{\epsilon}(|\vec{q}|), \quad (6)$$

where this time $\tilde{\epsilon}$ is given by

$$\tilde{\epsilon}(|\vec{q}|) \approx \frac{1}{6} \sum_f Q_{Z'}^f e_f \ln \left(\frac{m_f^2}{\Lambda^2} \right), \quad (7)$$

where f runs over μ/τ and all quarks. The couplings $Q_{Z'}^f$ are given in Tab. I and e_f denotes the electric charge of fermion f . Finally, Λ is the renormalization scale. While an accurate determination would require the full RGE running that is out of the scope of this work, for the sake of simplicity we fix $\Lambda = m_\mu$ (m_τ) in the case of $B - 3L_\mu$ ($B - 3L_\tau$). We have checked that by choosing a different scale, e.g. $\Lambda = 10^6$ GeV, $|\tilde{\epsilon}|$ would change by a factor of around 4 thus resulting in a bound a factor of 2 stronger.

III. DATA ANALYSIS

In this section, we present the analysis details for the experiments under consideration. Specifically, we discuss the analysis of current experiments (XENONnT, LZ and PandaX-4T) in subsection III A and the sensitivity for a next-generation detector, that we model following the DARWIN proposal [22], in subsection III B. The analysis procedure follows very closely the one described in Ref. [29].

² For the sake of completeness let us stress that for the case of $\text{CE}\nu\text{NS}$ there is a plus sign before the second term in Eq. (4) because of the different electric charge of protons versus electrons (see Ref. [71]).

A. Current experiments

Regarding current experiments we analyze data from LZ [9], XENONnT [6] and PandaX-4T [11]. The current energy threshold for $E\nu$ ES in these experiments is set at $E_{\text{thr}} = 1$ keV, although due to the detector efficiency the actual flux becomes sizable at ~ 3 keV. For each experiment the number of events due to elastic scattering of solar neutrinos is obtained through the following expression

$$R_k^{\text{E}\nu\text{ES}} = \mathcal{N} \int_{T_e^k}^{T_e^{k+1}} dT_e A(T_e) \int_0^{T_e^{\text{max}}} dT_e' R(T_e, T_e') \sum_{i=pp, {}^7\text{Be}} \int_{E_\nu^{\text{min}}}^{E_\nu^{\text{max}}} dE_\nu \sum_\alpha \Phi_{\nu_\alpha}^i(E_\nu) \frac{d\sigma_{\nu_\alpha A}}{dT_e'} . \quad (8)$$

Here, T_e and T_e' are the reconstructed and true electron recoil energies, respectively. The minimal neutrino energy necessary to produce an electron recoil of T_e' is given by $E_\nu^{\text{min}} = (T_e' + \sqrt{2m_e T_e' + T_e'^2})/2$, while the maximal neutrino energy E_ν^{max} is the energy endpoint of the production process inside the Sun, indicated with the index i ($i = pp, {}^7\text{Be}$). The recoil energy upper limit is given by kinematics: $T_e^{\text{max}} = 2E_\nu^2/(2E_\nu + m_e)$. The $E\nu$ ES cross section for a given neutrino flavor ν_α is given by $d\sigma_{\nu_\alpha A}/dT_e'$ and has been discussed in Section II. The fluxes $\Phi_{\nu_\alpha}^i(E_\nu)$ are given by

$$\Phi_{\nu_e}^i = \Phi_{\nu_e}^{i\odot} P_{ee}, \quad \Phi_{\nu_\mu}^i = \Phi_{\nu_e}^{i\odot} (1 - P_{ee}) \cos^2 \vartheta_{23}, \quad \Phi_{\nu_\tau}^i = \Phi_{\nu_e}^{i\odot} (1 - P_{ee}) \sin^2 \vartheta_{23}, \quad (9)$$

where $\Phi_{\nu_e}^{i\odot}$ are the fluxes of ν_e produced by thermonuclear reactions in the interior of the Sun, with $i = pp, {}^7\text{Be}$, etc. indicating the production reaction. For those, we employ the spectra from Refs. [74–77] with the normalizations for the high metallicity model taken from Ref. [78]. As anticipated, the main contributions relevant for the signal at the experiments under consideration originate from pp and ${}^7\text{Be}$ neutrinos. Moreover, P_{ee} is the ν_e -survival probability at the detector on Earth, accounting for neutrino oscillations. As can be seen, the fluxes of ν_μ and ν_τ depend on the mixing angle ϑ_{23} , which is close to maximal mixing ($\vartheta_{23} \sim \pi/4$) [79–81]. For simplicity, we consider $\sin^2 \vartheta_{23} = 0.5$, which implies $\Phi_{\nu_\mu}^i = \Phi_{\nu_\tau}^i$.

Next, $R(T_e, T_e')$ and $A(T_e)$ are the detector resolution and efficiency functions which are different for all experiments. We use the detector efficiencies given in Refs. [6, 11, 82]. For the energy resolution at LZ we use the same function that has been used in Refs. [27, 40]. In the case of XENONnT we use the resolution function of Ref. [83] and for PandaX-4T we use the one from Ref. [11]. Finally, $\mathcal{N} = \mathcal{E}N_T$ is a normalization constant which takes into account the exposure $\mathcal{E} = \{1.16, 0.90, 0.63\}$ ton \times year for XENONnT, LZ and PandaX-4T, respectively, while $N_T = N_A/M(\text{Xe})$ denotes the number of target nuclei per ton of detector material, N_A and $M(\text{Xe})$ being the Avogadro number and the molar mass of xenon.

The overall predicted number of events in a given energy-bin k for an experiment X is given by

$$R_k^X = R_k^{\text{E}\nu\text{ES}} + \sum_i R_k^i, \quad (10)$$

where $R_k^{\text{E}\nu\text{ES}}$ is the $E\nu$ ES contribution, Eq. (8), while R_k^i are the remaining background components of each experiment, extracted from Refs. [6, 11, 84] for LZ, XENONnT and PandaX-4T, respectively. The total number of predicted events has to be compared with the data D^X collected in each experiment. In our analyses we use the data from Fig. 6 of Ref. [9] for LZ and the data from Fig. 3 of Ref. [11] for PandaX-4T. In the case of XENONnT we use the data from Fig. 4 (5) of Ref. [6], for recoil energies above (below) 30 keV.

Due to the low statistics in some bins, for LZ and PandaX-4T we use the Poissonian least-squares function

$$\chi_X^2 = \min_{\vec{\alpha}, \vec{\beta}} \left\{ 2 \left(\sum_k R_k^X - D_k^X + D_k^X \ln \left(D_k^X / R_k^X \right) \right) + \sum_i (\alpha_i / \sigma_{\alpha_i})^2 + \sum_i (\beta_i / \sigma_{\beta_i})^2 \right\}, \quad (11)$$

where α_i are normalization constants multiplied to each single background component in Eq. (10), penalized by the uncertainties σ_{α_i} . These uncertainties are taken from Tab. VI of Ref. [84] for LZ and Tab. I of Ref. [11] for PandaX-4T. As indicated in the references, some of these nuisance parameters are left to vary freely in the analysis. Also included are the uncertainty coefficients β_i of the solar neutrino fluxes, with uncertainties σ_{β_i} taken from Ref. [78].

In the case of XENONnT data, we use instead

$$\chi_{\text{XENONnT}}^2 = \min_{\vec{\alpha}, \vec{\beta}} \left\{ \sum_k \left(\frac{R_k^{\text{XENONnT}} - D_k^{\text{XENONnT}}}{\sigma_k} \right)^2 + \sum_i (\alpha_i / \sigma_{\alpha_i})^2 + \sum_i (\beta_i / \sigma_{\beta_i})^2 \right\}, \quad (12)$$

where the uncertainties in each bin σ_k are extracted from Ref. [6]. The remaining components are equivalent to the corresponding ones for LZ and PandaX-4T.

We also perform a combined analysis of all three experiments by correlating the uncertainties regarding the neutrino flux among the experiments. In addition, background components which are common to at least two of the three experiments are also correlated.

B. DARWIN sensitivity

The calculation of the event rate at a future experiment like DARWIN is essentially the same as for the current experiments, given in Eqs. (8) and (10). The only difference is that we also include the contributions from solar N, O and *pep* neutrinos. It should be noted, however, that their contribution is mostly negligible in comparison with some of the background contributions, as shown in Fig. 1 of Ref. [22]. We include them, nevertheless, since we use the full spectrum as shown in Ref. [22].

The individual background components relevant for DARWIN are given in Ref. [22], and need to be normalized to the considered exposure. We use the same resolution function and detector efficiency as for XENONnT assuming that the efficiency remains constant for $T_e > T_{e,\text{max}}^{\text{XENONnT}}$. With these assumptions, we are able to reproduce the $E\nu\text{ES}$ spectra for all five neutrino species in Fig. 1 of Ref. [22], which justifies the choices of efficiency and resolution functions. We compute the sensitivity considering an exposure of 30 ton \times years and 300 ton \times years.

When generating the mock data, always compatible with the SM expectation, we use 51 logarithmically-spaced bins between 1 and 1500 keV recoil energy. Note that the spectrum at higher energies ($\gtrsim 700$ keV) is not sensitive to any BSM effect considered in this paper, because the $E\nu\text{ES}$ rate is much smaller than some of the background rates. Indeed, the main $E\nu\text{ES}$ rate contributions from *pp* and ${}^7\text{Be}$ neutrinos become irrelevant at $T_e \sim 250$ keV and ~ 700 keV, respectively. We still use the full spectrum up to 1500 keV, since the inclusion of events at high energies can help to control the effect of background uncertainties.

IV. RESULTS

In this section we present the bounds obtained for all models discussed in Section II. In all cases we compare our bounds with previous ones obtained in the literature, in particular with the ones included in the DarkCast package [85], the ones obtained from COHERENT data [54, 68] and from neutrino oscillation experiments [46]. DarkCast implements constraints from several classes of experiments³: beam dump (E141 [86], E137 [87], E774 [88], KEK [89], Orsay [90–92], ν -CAL I [93–96], CHARM [97, 98], NOMAD [99], and PS191 [100, 101]), fixed target (A1 [102] and APEX [103]),

³ Note that even though not all DarkCast bounds are at the same confidence level, small differences in confidence level are basically invisible on the scales of our plots.

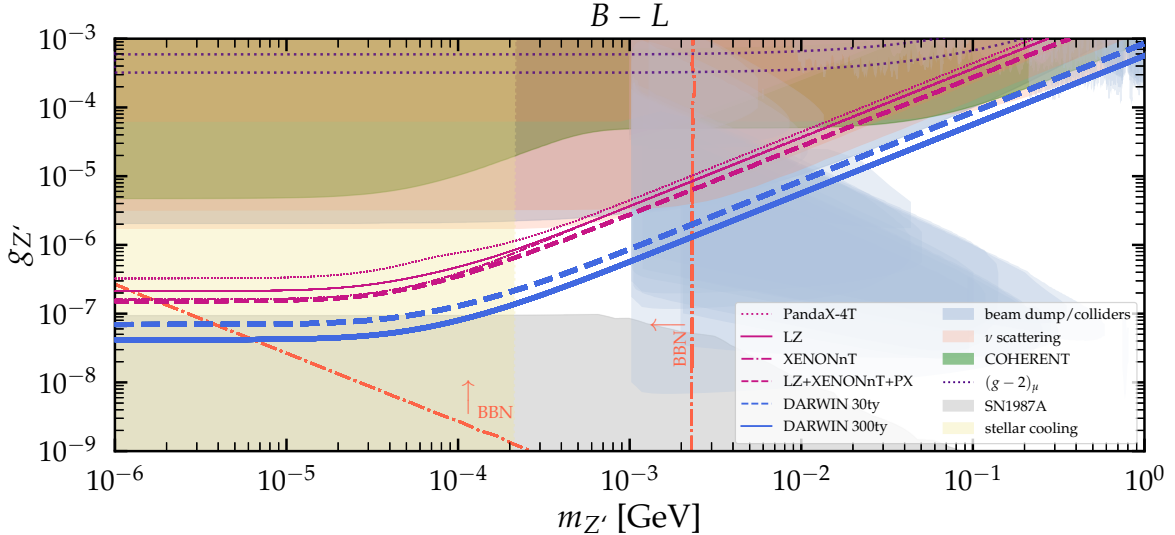


FIG. 1: 90% C.L. bounds from our analyses of: LZ (magenta solid), PandaX-4T (magenta dotted) and XENONnT data (magenta dashed-dotted), a combined analysis of current data (magenta dashed) and expected sensitivity at DARWIN with an exposure of 30 (blue dashed) or 300 ton \times years (blue solid) for the $B - L$ model, in comparison with other existing bounds.

colliders (BaBar [104], KLOE [105, 106], LHCb [107]), rare-meson decay (NA48/2 [108]) experiments, neutrino scattering experiments (TEXONO, CHARM-II and BOREXINO [109–113]), and searches for dark photons in NA64 [114–117] and BaBar [118].

The $B - L$ model

The 90% C.L. exclusion limits in the $m_{Z'} - g_{Z'}$ plane for the $B - L$ model are shown in Fig. 1. Our present results for XENONnT and LZ are in excellent agreement with a previous analysis performed in Ref. [40], though here the analysis is improved following the method of Ref. [29], as explained previously. The thin magenta lines correspond to the analyses of PandaX-4T (dotted), LZ (solid) and XENONnT (dashed-dotted) data, while the thick magenta dashed line is the result from our combined analysis⁴. At large (small) masses the dominating contribution to the bound comes from LZ (XENONnT) data. Note that since we correlated common uncertainties among the experiments, the combined bound is stronger than a simple sum of χ^2 functions. For low mediator masses ($\lesssim 0.1$ MeV), our combined limit saturates at $g_{Z'} \sim 1.5 \times 10^{-7}$.

As can be seen in Fig. 1, current DM DD experiments produce slightly weaker (stronger) bounds for large (small) masses than other experiments measuring $E\nu$ ES [109–113], like TEXONO, CHARM-II and BOREXINO (“ ν scattering”, depicted as coral-shaded areas). On the other hand, DM DD bounds do improve upon $CE\nu$ NS constraints⁵ from the COHERENT experiment [68] (green area), by about two orders of magnitude at $m_{Z'} \lesssim 0.01$ MeV. Among beam-dump experiments, usually covering masses $m_{Z'} \gtrsim 1$ MeV, let us highlight NA64 [115], whose bound applies to lighter mediators as well and is comparable to the limits set by ν -scattering experiments. It should be noted that current bounds from DM experiments are never dominating in comparison to

⁴ In order to not overcrowd the figures we will show only the combined result in subsequent figures.

⁵ Note that the depicted constraints actually include $CE\nu$ NS+ $E\nu$ ES events in the analysis of COHERENT-CsI data (see Refs. [66, 68] for details).

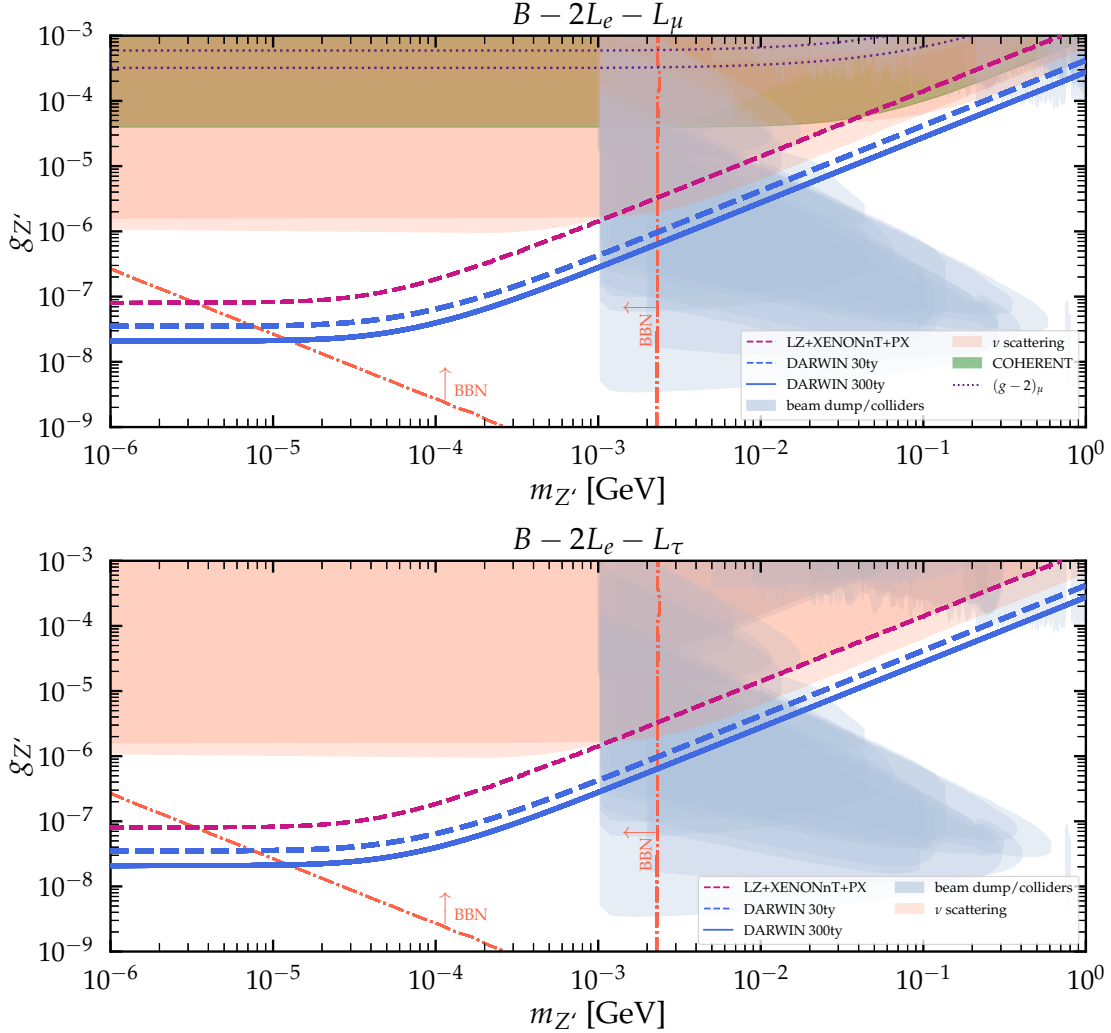


FIG. 2: 90% C.L. bounds from our combined analysis of LZ, PandaX-4T and XENONnT data and the sensitivity at DARWIN for the $B - 2L_e - L_\mu$ (upper panel) and $B - 2L_e - L_\tau$ (lower panel) models. Also shown are bounds from other experiments for comparison.

other probes for large mediator masses, i.e., $m_{Z'} \gtrsim 10$ MeV. However, DARWIN will provide the dominating bounds in the region $0.02 \text{ GeV} \lesssim m_{Z'} \lesssim 0.4 \text{ GeV}$, between the blue- and coral-shaded regions corresponding to beam-dump and accelerator experiments and scattering experiments, respectively. The purple dotted lines indicate the region of parameter space that could explain the $(g-2)_\mu$ anomaly [119] and that is therefore now excluded by several experiments. Let us finally note that below the \sim MeV scale strong bounds from big bang nucleosynthesis [120] (orange dashed-dotted lines) and stellar cooling [121] effects (yellow area) apply, although their exact estimation will eventually depend on the specific model and thermal history in the early Universe. Finally, bounds from SN1987A [122, 123] (light gray) constrain the region in the plot for small couplings⁶.

⁶ Let us note that the latter constraints might be less stringent as explained in Refs. [124, 125].

The $B - 2L_e - L_{\mu/\tau}$ models

The upper (lower) panel of Fig. 2 shows the results for the $B - 2L_e - L_{\mu}$ ($B - 2L_e - L_{\tau}$) models [53, 54]. Due to our choice of $\sin^2 \theta_{23} = 0.5$ the bounds from DM DD experiments are the same for both models. However, the bounds from other experiments can change. Note that although not analyzed in Ref. [54], COHERENT data could also be used to place bounds on the $B - 2L_e - L_{\tau}$ scenario, however the resulting limit would be slightly weaker than those for $B - 2L_e - L_{\mu}$ and definitely weaker than our combined constraint from LZ+PandaX-4T+XENONnT. As in the previous case of the $B - L$ model, solar ν ES data at DM DD experiments will be able to provide the dominating bound in the $0.02 \text{ GeV} \lesssim m_{Z'} \lesssim 0.2 \text{ GeV}$ mass region even after a relatively short exposure time at DARWIN, while the current limit (magenta dashed) is slightly weaker than other probes, but nonetheless comparable to other limits from neutrino scattering at $m_{Z'} \gtrsim 1 \text{ MeV}$. All in all, at small masses $m_{Z'} \lesssim 1 \text{ MeV}$ the bounds from DM DD experiments are significantly stronger than those from other laboratory probes, while being surpassed by astrophysical and cosmological observations.

The $B - 3L_{\alpha}$ models

We next discuss the results obtained for the $B - 3L_{\alpha}$ models. Results are presented in Fig. 3. In the case of $B - 3L_e$ we find a behavior that resembles previous models. At large mediator masses current DM DD experiments are slightly weaker than other probes, while DARWIN has the prospect to provide the leading bound in the future. At small masses our bounds are the strongest limits obtained using neutrino fluxes in some parts of the parameter space. However, the bound from oscillation experiments [46] (light lavender) starts to dominate for mediator masses below $\sim \mathcal{O}(10) \text{ keV}$.

In the second and third row of Fig. 3 we show the results for the $B - 3L_{\mu}$ and $B - 3L_{\tau}$ models, respectively. We focus on a reduced range of mediator masses, since for smaller masses a more thorough treatment of the loop-effects in Eq. (7) might become necessary. As can be seen, our bounds from current DM DD experiments as well as the projected sensitivity for DARWIN seem not to be competitive with oscillation experiments. The reason is that these models affect the ν ES process only at the loop-level and hence the overall effect on the cross section is very tiny in comparison with the $B - 3L_e$ model, for which the interaction occurs instead at tree level.

The $L_{\alpha} - L_{\beta}$ models

In the last two subsections we discuss models that only couple to leptons. We start with the $L_{\alpha} - L_{\beta}$ models. Our results are presented in Fig. 4. As in previous cases, we find that DARWIN will be able to provide the dominant bound in some regions of the parameter space, even with relatively small exposure, for $L_e - L_{\mu/\tau}$. For the same symmetry arguments already mentioned above, our bounds and sensitivities are the same for both models. Even though DARWIN will provide the strongest bound at large mediator masses, at small masses the bounds from oscillation experiments remain very strong as can be seen in Fig. 4.

In the case of the $L_{\mu} - L_{\tau}$ model, current bounds from DM DD experiments are of similar strength as those from other ν ES probes (“ ν scattering”) and are expected to become much stronger once DARWIN starts taking data. The current combined limit already rules out $L_{\mu} - L_{\tau}$ as an explanation to the $(g - 2)_{\mu}$ anomaly, at $m_{Z'} \lesssim 100 \text{ MeV}$. Notice also that at $m_{Z'} \gtrsim 100 \text{ MeV}$ the NA64 bound [117] becomes relevant and excludes couplings $g_{Z'} \gtrsim 5 \times 10^{-3}$. We do not show oscillation bounds for this model, because this scenario was not considered in Ref. [46]. The

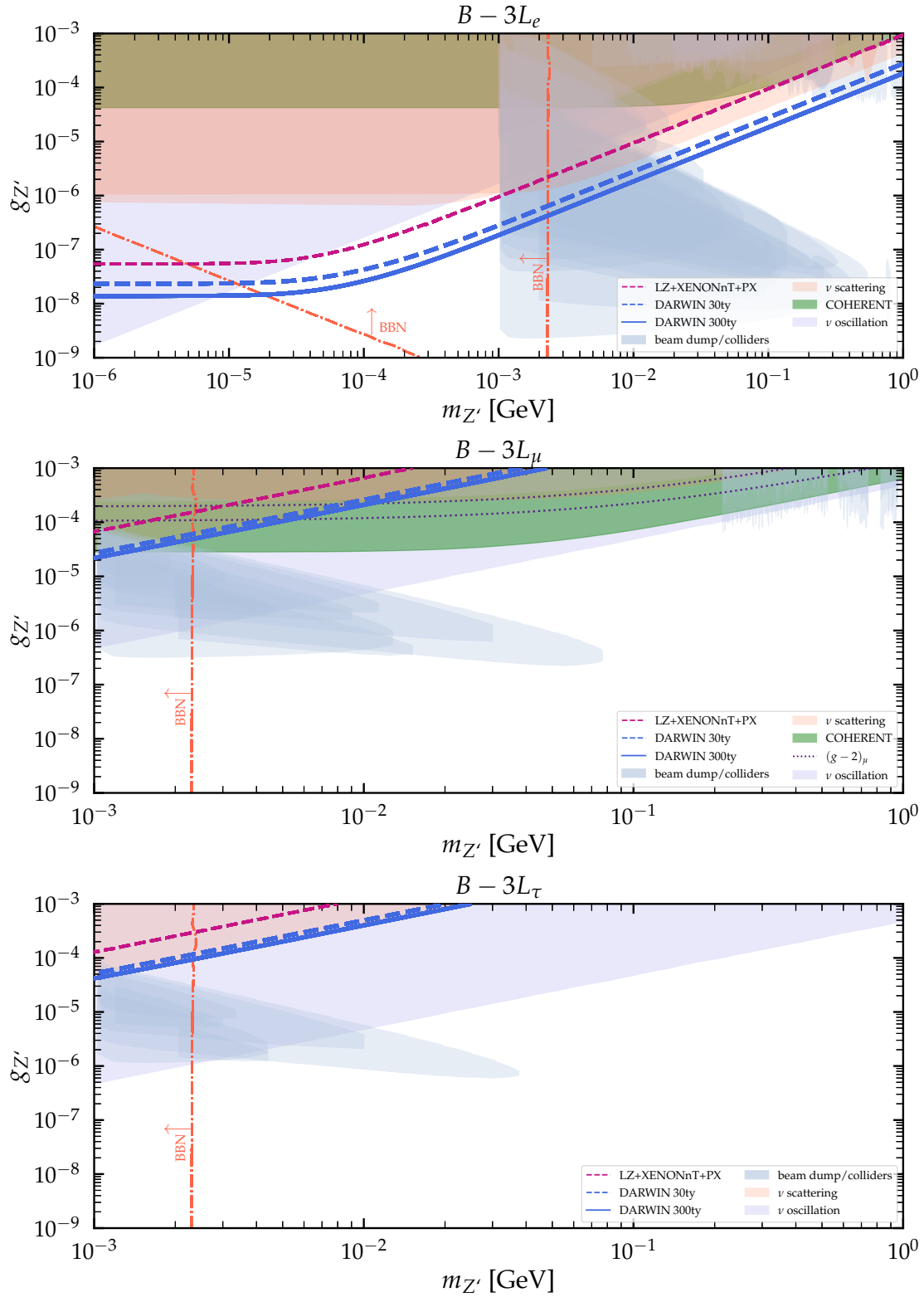


FIG. 3: The bounds from our combined analysis of LZ, PandaX-4T and XENONnT data and the sensitivity at DARWIN at 90% C.L. for $B - 3L_e$ (first row), $B - 3L_\mu$ (second row) and $B - 3L_\tau$ (third row). Also shown are bounds from other experiments for comparison.

COHERENT result, available for the case of $L_\mu - L_\tau$ only, is taken from Ref. [68]⁷. Let us also mention that bounds for very small mediator masses have been calculated in Ref. [126]. However, for the mass range of interest in this work, those bounds are many orders of magnitude weaker than the ones derived in this work. Finally, a large region of parameter space with small coupling is in conflict with cosmological observations [127] (ΔN_{eff}) and supernova data [123, 128, 129].

The $L_e + 2L_\mu + 2L_\tau$ model

The last model that we consider is $L_e + 2L_\mu + 2L_\tau$. The results are shown in Fig. 5. As in the case of previous models we find that DM DD experiments currently provide limits comparable to other $\nu - e^-$ scattering experiments but will improve in some parts of the parameter space with future facilities like DARWIN. For low mediator masses, however, DM DD bounds are already much stronger than the ones obtained from other experiments using $E\nu\text{ES}$ and will be further improved by DARWIN. As in previous scenarios, these bounds probe parts of the parameter space in complementarity to those probed by astrophysical observations or by other terrestrial experiments like beam dump and colliders.

V. CONCLUSIONS

The large exposures achieved at recent dark matter direct detection experiments, combined with the very low threshold operation capabilities of recent LXe and future LAr detectors, mark a turning point in solar neutrino detection. Motivated by this unique opportunity, we have performed a thorough analysis of compelling $U(1)'$ models, by analyzing current (XENONnT, LZ and PandaX-4T) and future (DARWIN) DM DD experiments via the $E\nu\text{ES}$ channel. In particular, we have focused on spectral distortions expected in the $E\nu\text{ES}$ rates that arise in the presence of novel interactions within the anomaly-free $B - L$, $L_\alpha - L_\beta$, $B - 2L_e - L_{\mu,\tau}$, $B - 3L_\alpha$, and $L_e + 2L_\mu + 2L_\tau$ models. By means of an improved statistical analysis, in which the various experimental uncertainties are treated separately, we have obtained stringent constraints on the relevant parameter space of the new vector mediator, $(m_{Z'}, g_{Z'})$. We have presented a combined analysis of ongoing experiments: XENONnT, LZ and PandaX-4T showing that it leads to slightly improved sensitivities compared to those obtained by analyzing each experiment individually. Specifically, we have shown that for $m_{Z'} \gtrsim 100$ MeV current DM DD experiments place competitive constraints, complementing other experimental probes including neutrino oscillation data, beam dump and collider searches. On the other hand, in the low mass regime i.e. for $m_{Z'} \lesssim 1$ MeV we have illustrated that the $E\nu\text{ES}$ channel dominates the constraints among terrestrial experiments. We have further shown that sensitivities achievable at future DM DD experiments like DARWIN—in view of their large size—will offer further improvements. We have finally discussed complementarities of our present results with constraints coming from astrophysical observations, especially those obtained from BBN and stellar cooling data.

ACKNOWLEDGMENTS

We thank Martin K. Hirsch for enlightening discussions, Sergei Gninenko, Laura Molina Bueno and Andrés D. Pérez for useful comments. V.D.R. acknowledges financial support by the CIDEXG/2022/20 grant (project “D’AMAGAT”) funded by Generalitat Valenciana and by

⁷ For $g_{Z'} < 10^{-3}$ the COHERENT bound is entirely driven by $E\nu\text{ES}$ events.

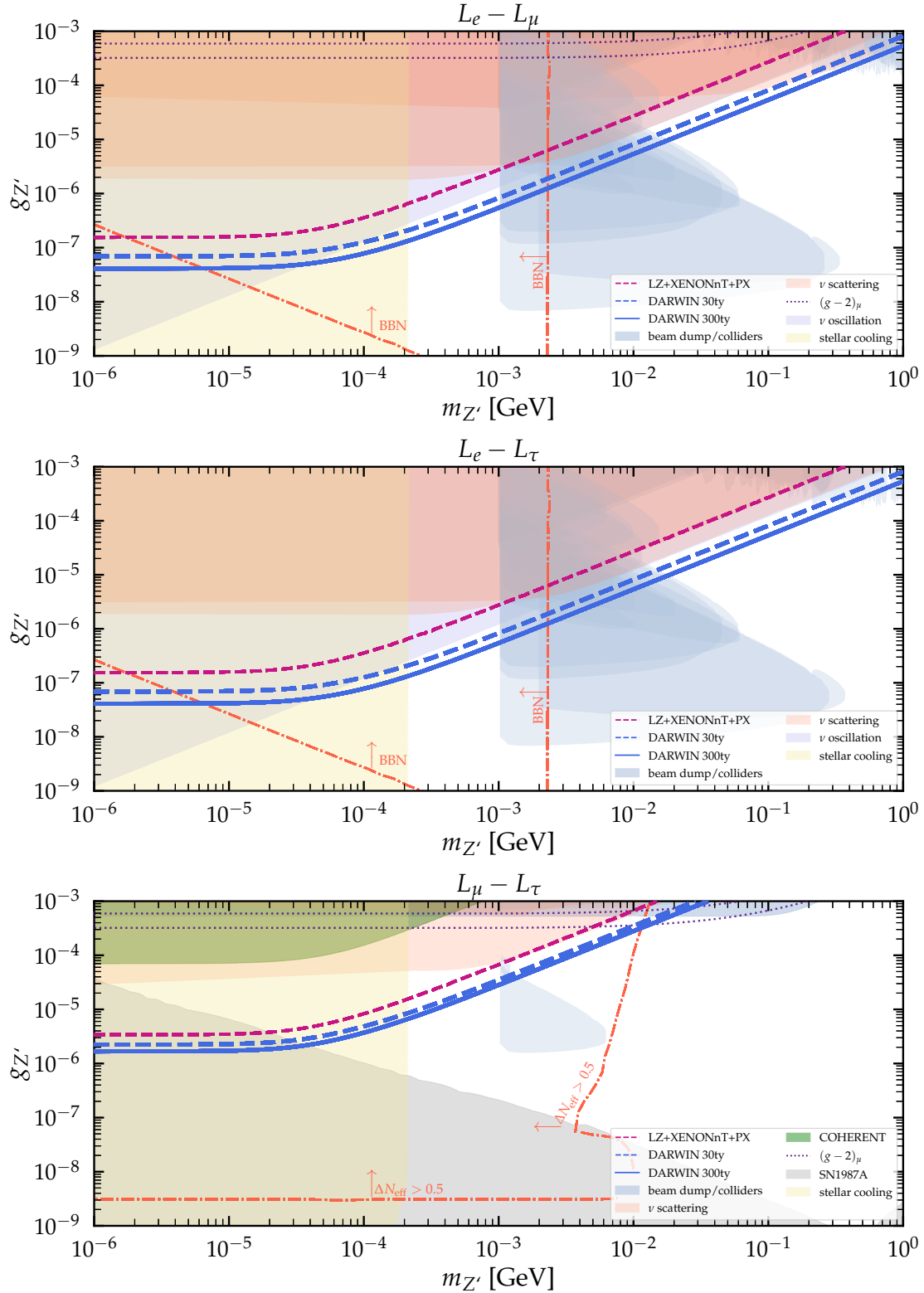


FIG. 4: The bounds from our combined analysis of LZ, PandaX-4T and XENONnT data and the sensitivity at DARWIN at 90% C.L. for $L_e - L_\mu$ (first row), $L_e - L_\tau$ (second row) and $L_\mu - L_\tau$ (third row). Also shown are bounds from other experiments for comparison.

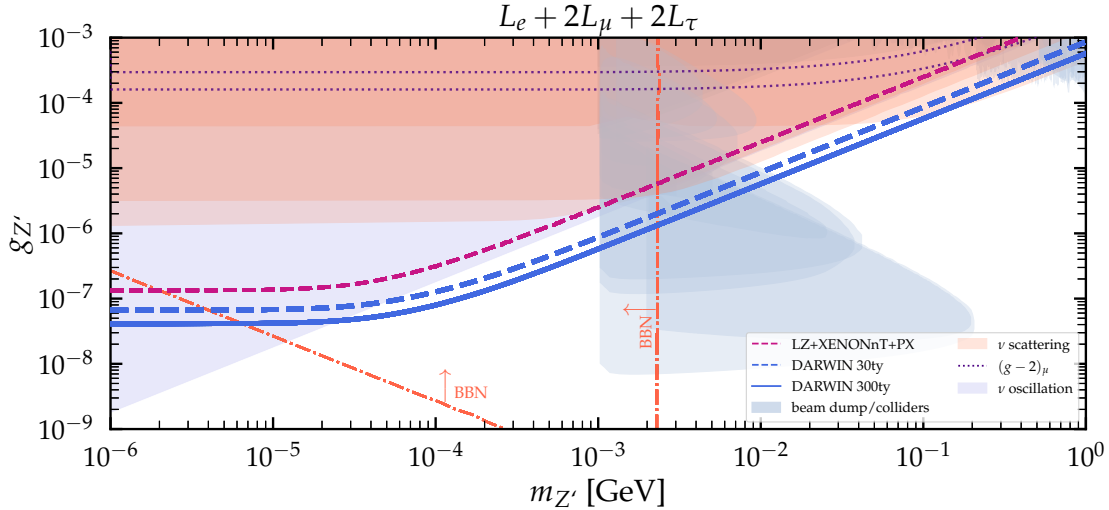


FIG. 5: The bounds from our combined analysis of LZ, PandaX-4T and XENONnT data and the sensitivity at DARWIN at 90% C.L. for $L_e + 2L_\mu + 2L_\tau$. Also shown are bounds from other experiments for comparison.

the Spanish grant PID2020-113775GB-I00 (MCIN/AEI/10.13039/501100011033). The work of DKP was supported by the Hellenic Foundation for Research and Innovation (H.F.R.I.) under the “3rd Call for H.F.R.I. Research Projects to support Post-Doctoral Researchers” (Project Number: 7036).

-
- [1] M. Schumann, “Direct Detection of WIMP Dark Matter: Concepts and Status,” *J. Phys. G* **46** no. 10, (2019) 103003, [arXiv:1903.03026 \[astro-ph.CO\]](#).
 - [2] D. Baxter *et al.*, “Recommended conventions for reporting results from direct dark matter searches,” *Eur. Phys. J. C* **81** no. 10, (2021) 907, [arXiv:2105.00599 \[hep-ex\]](#).
 - [3] J. Billard *et al.*, “Direct detection of dark matter—APPEC committee report*,” *Rept. Prog. Phys.* **85** no. 5, (2022) 056201, [arXiv:2104.07634 \[hep-ex\]](#).
 - [4] XENON Collaboration, E. Aprile *et al.*, “The XENON1T Dark Matter Experiment,” *Eur. Phys. J. C* **77** no. 12, (2017) 881, [arXiv:1708.07051 \[astro-ph.IM\]](#).
 - [5] XENON Collaboration, E. Aprile *et al.*, “Dark Matter Search Results from a One Ton-Year Exposure of XENON1T,” *Phys. Rev. Lett.* **121** no. 11, (2018) 111302, [arXiv:1805.12562 \[astro-ph.CO\]](#).
 - [6] XENON Collaboration, E. Aprile *et al.*, “Search for New Physics in Electronic Recoil Data from XENONnT,” *Phys. Rev. Lett.* **129** no. 16, (2022) 161805, [arXiv:2207.11330 \[hep-ex\]](#).
 - [7] LZ Collaboration, D. S. Akerib *et al.*, “LUX-ZEPLIN (LZ) Conceptual Design Report,” [arXiv:1509.02910 \[physics.ins-det\]](#).
 - [8] LZ Collaboration, D. S. Akerib *et al.*, “The LUX-ZEPLIN (LZ) Experiment,” *Nucl. Instrum. Meth. A* **953** (2020) 163047, [arXiv:1910.09124 \[physics.ins-det\]](#).
 - [9] LZ Collaboration, J. Aalbers *et al.*, “First Dark Matter Search Results from the LUX-ZEPLIN (LZ) Experiment,” *Phys. Rev. Lett.* **131** no. 4, (2023) 041002, [arXiv:2207.03764 \[hep-ex\]](#).
 - [10] PandaX Collaboration, X. Cao *et al.*, “PandaX: A Liquid Xenon Dark Matter Experiment at CJPL,” *Sci. China Phys. Mech. Astron.* **57** (2014) 1476–1494, [arXiv:1405.2882 \[physics.ins-det\]](#).
 - [11] PandaX Collaboration, D. Zhang *et al.*, “Search for Light Fermionic Dark Matter Absorption on Electrons in PandaX-4T,” *Phys. Rev. Lett.* **129** no. 16, (2022) 161804, [arXiv:2206.02339 \[hep-ex\]](#).
 - [12] PandaX Collaboration, A. Abdulkarim *et al.*, “PandaX-xT: a Multi-ten-tonne Liquid Xenon Observatory at the China Jinping Underground Laboratory,” [arXiv:2402.03596 \[hep-ex\]](#).

- [13] T. Bringmann and M. Pospelov, “Novel direct detection constraints on light dark matter,” *Phys. Rev. Lett.* **122** no. 17, (2019) 171801, [arXiv:1810.10543 \[hep-ph\]](#).
- [14] V. De Romeri, A. Majumdar, D. K. Papoulias, and R. Srivastava, “XENONnT and LUX-ZEPLIN constraints on DSNB-boosted dark matter,” [arXiv:2309.04117 \[hep-ph\]](#).
- [15] I. M. Bloch, A. Caputo, R. Essig, D. Redigolo, M. Sholapurkar, and T. Volansky, “Exploring new physics with O(keV) electron recoils in direct detection experiments,” *JHEP* **01** (2021) 178, [arXiv:2006.14521 \[hep-ph\]](#).
- [16] R. Z. Ferreira, M. C. D. Marsh, and E. Müller, “Do Direct Detection Experiments Constrain Axionlike Particles Coupled to Electrons?,” *Phys. Rev. Lett.* **128** no. 22, (2022) 221302, [arXiv:2202.08858 \[hep-ph\]](#).
- [17] H. An, M. Pospelov, J. Pradler, and A. Ritz, “Direct Detection Constraints on Dark Photon Dark Matter,” *Phys. Lett. B* **747** (2015) 331–338, [arXiv:1412.8378 \[hep-ph\]](#).
- [18] J. A. Dror, G. Elor, and R. McGehee, “Absorption of Fermionic Dark Matter by Nuclear Targets,” *JHEP* **02** (2020) 134, [arXiv:1908.10861 \[hep-ph\]](#).
- [19] **(XENON Collaboration)**§, XENON Collaboration, E. Aprile *et al.*, “Search for events in XENON1T associated with gravitational waves,” *Phys. Rev. D* **108** no. 7, (2023) 072015, [arXiv:2306.11871 \[hep-ex\]](#).
- [20] R. Essig *et al.*, “Snowmass2021 Cosmic Frontier: The landscape of low-threshold dark matter direct detection in the next decade,” in *Snowmass 2021*. 3, 2022. [arXiv:2203.08297 \[hep-ph\]](#).
- [21] D. S. Akerib *et al.*, “Snowmass2021 Cosmic Frontier Dark Matter Direct Detection to the Neutrino Fog,” in *Snowmass 2021*. 3, 2022. [arXiv:2203.08084 \[hep-ex\]](#).
- [22] **DARWIN** Collaboration, J. Aalbers *et al.*, “Solar neutrino detection sensitivity in DARWIN via electron scattering,” *Eur. Phys. J. C* **80** no. 12, (2020) 1133, [arXiv:2006.03114 \[physics.ins-det\]](#).
- [23] J. Aalbers *et al.*, “A next-generation liquid xenon observatory for dark matter and neutrino physics,” *J. Phys. G* **50** no. 1, (2023) 013001, [arXiv:2203.02309 \[physics.ins-det\]](#).
- [24] **DarkSide-20k** Collaboration, V. Pesudo, “Measurement of the underground argon radiopurity for Dark Matter direct searches,” *J. Phys. Conf. Ser.* **2156** no. 1, (2021) 012043.
- [25] J. Billard, L. Strigari, and E. Figueroa-Feliciano, “Implication of neutrino backgrounds on the reach of next generation dark matter direct detection experiments,” *Phys. Rev. D* **89** no. 2, (2014) 023524, [arXiv:1307.5458 \[hep-ph\]](#).
- [26] C. A. J. O’Hare, “New Definition of the Neutrino Floor for Direct Dark Matter Searches,” *Phys. Rev. Lett.* **127** no. 25, (2021) 251802, [arXiv:2109.03116 \[hep-ph\]](#).
- [27] M. Atzori Corona, W. M. Bonivento, M. Cadeddu, N. Cargioli, and F. Dordei, “New constraint on neutrino magnetic moment and neutrino millicharge from LUX-ZEPLIN dark matter search results,” *Phys. Rev. D* **107** no. 5, (2023) 053001, [arXiv:2207.05036 \[hep-ph\]](#).
- [28] A. de Gouvêa, E. McGinness, I. Martinez-Soler, and Y. F. Perez-Gonzalez, “pp solar neutrinos at DARWIN,” *Phys. Rev. D* **106** no. 9, (2022) 096017, [arXiv:2111.02421 \[hep-ph\]](#).
- [29] C. Giunti and C. A. Ternes, “Testing neutrino electromagnetic properties at current and future dark matter experiments,” *Phys. Rev. D* **108** no. 9, (2023) 095044, [arXiv:2309.17380 \[hep-ph\]](#).
- [30] D. G. Cerdeño, M. Fairbairn, T. Jubb, P. A. N. Machado, A. C. Vincent, and C. Boehm, “Physics from solar neutrinos in dark matter direct detection experiments,” *JHEP* **05** (2016) 118, [arXiv:1604.01025 \[hep-ph\]](#). [Erratum: *JHEP* 09, 048 (2016)].
- [31] B. Dutta, S. Liao, L. E. Strigari, and J. W. Walker, “Non-standard interactions of solar neutrinos in dark matter experiments,” *Phys. Lett. B* **773** (2017) 242–246, [arXiv:1705.00661 \[hep-ph\]](#).
- [32] G. B. Gelmini, V. Takhistov, and S. J. Witte, “Geoneutrinos in Large Direct Detection Experiments,” *Phys. Rev. D* **99** no. 9, (2019) 093009, [arXiv:1812.05550 \[hep-ph\]](#).
- [33] R. Essig, M. Sholapurkar, and T.-T. Yu, “Solar Neutrinos as a Signal and Background in Direct-Detection Experiments Searching for Sub-GeV Dark Matter With Electron Recoils,” *Phys. Rev. D* **97** no. 9, (2018) 095029, [arXiv:1801.10159 \[hep-ph\]](#).
- [34] D. W. P. d. Amaral, D. G. Cerdeno, P. Foldenauer, and E. Reid, “Solar neutrino probes of the muon anomalous magnetic moment in the gauged $U(1)_{L_\mu-L_\tau}$,” *JHEP* **12** (2020) 155, [arXiv:2006.11225 \[hep-ph\]](#).
- [35] B. Dutta, R. F. Lang, S. Liao, S. Sinha, L. Strigari, and A. Thompson, “A global analysis strategy to resolve neutrino NSI degeneracies with scattering and oscillation data,” *JHEP* **09** (2020) 106,

- [arXiv:2002.03066 \[hep-ph\]](#).
- [36] D. W. P. Amaral, D. G. Cerdeno, A. Cheek, and P. Foldenauer, “Confirming $U(1)_{L_\mu-L_\tau}$ as a solution for $(g-2)_\mu$ with neutrinos,” *Eur. Phys. J. C* **81** no. 10, (2021) 861, [arXiv:2104.03297 \[hep-ph\]](#).
- [37] V. Munoz, V. Takhistov, S. J. Witte, and G. M. Fuller, “Exploring the origin of supermassive black holes with coherent neutrino scattering,” *JCAP* **11** no. 11, (2021) 020, [arXiv:2102.00885 \[astro-ph.HE\]](#).
- [38] J. Wyenberg and I. M. Shoemaker, “Mapping the neutrino floor for direct detection experiments based on dark matter-electron scattering,” *Phys. Rev. D* **97** no. 11, (2018) 115026, [arXiv:1803.08146 \[hep-ph\]](#).
- [39] D. Aristizabal Sierra, V. De Romeri, L. J. Flores, and D. K. Papoulias, “Impact of COHERENT measurements, cross section uncertainties and new interactions on the neutrino floor,” *JCAP* **01** no. 01, (2022) 055, [arXiv:2109.03247 \[hep-ph\]](#).
- [40] S. K. A., A. Majumdar, D. K. Papoulias, H. Prajapati, and R. Srivastava, “Implications of first LZ and XENONnT results: A comparative study of neutrino properties and light mediators,” *Phys. Lett. B* **839** (2023) 137742, [arXiv:2208.06415 \[hep-ph\]](#).
- [41] N. Mishra and L. E. Strigari, “Solar neutrinos with $CE\nu$ NS and flavor-dependent radiative corrections,” *Phys. Rev. D* **108** no. 6, (2023) 063023, [arXiv:2305.17827 \[hep-ph\]](#).
- [42] D. W. P. Amaral, D. Cerdeno, A. Cheek, and P. Foldenauer, “A direct detection view of the neutrino NSI landscape,” *JHEP* **07** (2023) 071, [arXiv:2302.12846 \[hep-ph\]](#).
- [43] P. Langacker, “The Physics of Heavy Z' Gauge Bosons,” *Rev. Mod. Phys.* **81** (2009) 1199–1228, [arXiv:0801.1345 \[hep-ph\]](#).
- [44] C. Boehm, D. G. Cerdeno, M. Fairbairn, P. A. N. Machado, and A. C. Vincent, “Light new physics in XENON1T,” *Phys. Rev. D* **102** (2020) 115013, [arXiv:2006.11250 \[hep-ph\]](#).
- [45] D. Aristizabal Sierra, V. De Romeri, L. J. Flores, and D. K. Papoulias, “Light vector mediators facing XENON1T data,” *Phys. Lett. B* **809** (2020) 135681, [arXiv:2006.12457 \[hep-ph\]](#).
- [46] P. Coloma, M. C. Gonzalez-Garcia, and M. Maltoni, “Neutrino oscillation constraints on $U(1)'$ models: from non-standard interactions to long-range forces,” *JHEP* **01** (2021) 114, [arXiv:2009.14220 \[hep-ph\]](#). [Erratum: *JHEP* 11, 115 (2022)].
- [47] R. N. Mohapatra, “From Old Symmetries to New Symmetries: Quarks, Leptons and B-L,” *Int. J. Mod. Phys. A* **29** no. 29, (2014) 1430066, [arXiv:1409.7557 \[hep-ph\]](#).
- [48] S. Okada, “ Z' Portal Dark Matter in the Minimal $B-L$ Model,” *Adv. High Energy Phys.* **2018** (2018) 5340935, [arXiv:1803.06793 \[hep-ph\]](#).
- [49] R. Foot, “New Physics From Electric Charge Quantization?,” *Mod. Phys. Lett. A* **6** (1991) 527–530.
- [50] R. Foot, G. C. Joshi, H. Lew, and R. R. Volkas, “Charge quantization in the standard model and some of its extensions,” *Mod. Phys. Lett. A* **5** (1990) 2721–2732.
- [51] R. Foot, H. Lew, and R. R. Volkas, “Electric charge quantization,” *J. Phys. G* **19** (1993) 361–372, [arXiv:hep-ph/9209259](#). [Erratum: *J.Phys.G* 19, 1067 (1993)].
- [52] X. G. He, G. C. Joshi, H. Lew, and R. R. Volkas, “NEW Z-prime PHENOMENOLOGY,” *Phys. Rev. D* **43** (1991) 22–24.
- [53] L. M. G. de la Vega, L. J. Flores, N. Nath, and E. Peinado, “Complementarity between dark matter direct searches and $CE\nu$ NS experiments in $U(1)'$ models,” *JHEP* **09** (2021) 146, [arXiv:2107.04037 \[hep-ph\]](#).
- [54] M. Atzori Corona, M. Cadeddu, N. Cargioli, F. Dordei, C. Giunti, Y. F. Li, E. Picciau, C. A. Ternes, and Y. Y. Zhang, “Probing light mediators and $(g-2)_\tau$ through detection of coherent elastic neutrino nucleus scattering at COHERENT,” *JHEP* **05** (2022) 109, [arXiv:2202.11002 \[hep-ph\]](#).
- [55] T. Han, J. Liao, H. Liu, and D. Marfatia, “Nonstandard neutrino interactions at COHERENT, DUNE, T2HK and LHC,” *JHEP* **11** (2019) 028, [arXiv:1910.03272 \[hep-ph\]](#).
- [56] J. Heeck, M. Lindner, W. Rodejohann, and S. Vogl, “Non-Standard Neutrino Interactions and Neutral Gauge Bosons,” *SciPost Phys.* **6** no. 3, (2019) 038, [arXiv:1812.04067 \[hep-ph\]](#).
- [57] B. Barman, P. Ghosh, A. Ghoshal, and L. Mukherjee, “Shedding flavor on dark via freeze-in: $U(1)_{B-3L_i}$ gauged extensions,” *JCAP* **08** no. 08, (2022) 049, [arXiv:2112.12798 \[hep-ph\]](#).
- [58] E. Ma, “Gauged $B-3L(\tau)$ and radiative neutrino masses,” *Phys. Lett. B* **433** (1998) 74–81, [arXiv:hep-ph/9709474](#).
- [59] E. Ma and D. P. Roy, “Phenomenology of the $B-3L(\tau)$ gauge boson,” *Phys. Rev. D* **58** (1998) 095005, [arXiv:hep-ph/9806210](#).

- [60] E. Ma and U. Sarkar, “Gauged B - 3L(tau) and baryogenesis,” *Phys. Lett. B* **439** (1998) 95–102, [arXiv:hep-ph/9807307](#).
- [61] E. Ma, D. P. Roy, and U. Sarkar, “A Seesaw model for atmospheric and solar neutrino oscillations,” *Phys. Lett. B* **444** (1998) 391–396, [arXiv:hep-ph/9810309](#).
- [62] L. N. Chang, O. Lebedev, W. Loinaz, and T. Takeuchi, “Constraints on gauged B - 3 L(tau) and related theories,” *Phys. Rev. D* **63** (2001) 074013, [arXiv:hep-ph/0010118](#).
- [63] A. N. Khan, “Constraints on general light mediators from PandaX-II electron recoil data,” *Phys. Lett. B* **819** (2021) 136415, [arXiv:2008.10279 \[hep-ph\]](#).
- [64] **PandaX-II** Collaboration, X. Zhou *et al.*, “A Search for Solar Axions and Anomalous Neutrino Magnetic Moment with the Complete PandaX-II Data,” *Chin. Phys. Lett.* **38** no. 1, (2021) 011301, [arXiv:2008.06485 \[hep-ex\]](#). [Erratum: *Chin.Phys.Lett.* 38, 109902 (2021)].
- [65] T. Schwemmer and T.-T. Yu, “Detecting beyond the standard model interactions of solar neutrinos in low-threshold dark matter detectors,” *Phys. Rev. D* **106** no. 1, (2022) 015002, [arXiv:2202.01254 \[hep-ph\]](#).
- [66] V. De Romeri, O. G. Miranda, D. K. Papoulias, G. Sanchez Garcia, M. Tórtola, and J. W. F. Valle, “Physics implications of a combined analysis of COHERENT CsI and LAr data,” *JHEP* **04** (2023) 035, [arXiv:2211.11905 \[hep-ph\]](#).
- [67] P. Coloma, M. C. Gonzalez-Garcia, M. Maltoni, J. a. P. Pinheiro, and S. Urrea, “Constraining new physics with Borexino Phase-II spectral data,” *JHEP* **07** (2022) 138, [arXiv:2204.03011 \[hep-ph\]](#). [Erratum: *JHEP* 11, 138 (2022)].
- [68] P. Melas, D. K. Papoulias, and N. Saoulidou, “Probing generalized neutrino interactions with the DUNE Near Detector,” *JHEP* **07** (2023) 190, [arXiv:2303.07094 \[hep-ph\]](#).
- [69] K. Asai, A. Das, J. Li, T. Nomura, and O. Seto, “Probing for chiral Z’ gauge boson through scattering measurement experiments,” *Phys. Rev. D* **109** no. 7, (2024) 075026, [arXiv:2307.09737 \[hep-ph\]](#).
- [70] J.-C. Park and G. Tomar, “Probing non-standard neutrino interactions with interference: insights from dark matter and neutrino experiments,” *JCAP* **08** (2023) 025, [arXiv:2305.10836 \[hep-ph\]](#).
- [71] A. Majumdar, D. K. Papoulias, and R. Srivastava, “Dark matter detectors as a novel probe for light new physics,” *Phys. Rev. D* **106** no. 1, (2022) 013001, [arXiv:2112.03309 \[hep-ph\]](#).
- [72] M. Demirci and M. F. Mustamin, “Solar neutrino constraints on light mediators through coherent elastic neutrino-nucleus scattering,” [arXiv:2312.17502 \[hep-ph\]](#).
- [73] J.-W. Chen, H.-C. Chi, C. P. Liu, and C.-P. Wu, “Low-energy electronic recoil in xenon detectors by solar neutrinos,” *Phys. Lett. B* **774** (2017) 656–661, [arXiv:1610.04177 \[hep-ex\]](#).
- [74] J. Bahcall. <http://www.sns.ias.edu/~jnb/SNdata/sndata.html>.
- [75] J. N. Bahcall and R. K. Ulrich, “Solar Models, Neutrino Experiments and Helioseismology,” *Rev. Mod. Phys.* **60** (1988) 297–372.
- [76] J. N. Bahcall, “The Be-7 solar neutrino line: A Reflection of the central temperature distribution of the sun,” *Phys. Rev. D* **49** (1994) 3923–3945, [arXiv:astro-ph/9401024](#).
- [77] J. N. Bahcall, E. Lisi, D. E. Alburger, L. De Braekeleer, S. J. Freedman, and J. Napolitano, “Standard neutrino spectrum from B-8 decay,” *Phys. Rev. C* **54** (1996) 411–422, [arXiv:nucl-th/9601044](#).
- [78] F. L. Villante and A. Serenelli, “The relevance of nuclear reactions for Standard Solar Models construction,” *Front. Astron. Space Sci.* **7** (2021) 112, [arXiv:2101.03077 \[astro-ph.SR\]](#).
- [79] P. F. de Salas, D. V. Forero, S. Gariazzo, P. Martinez-Mirave, O. Mena, C. A. Ternes, M. Tortola, and J. W. F. Valle, “2020 Global reassessment of the neutrino oscillation picture,” *JHEP* **2021** (2020) 071, [arXiv:2006.11237 \[hep-ph\]](#).
- [80] I. Esteban, M. C. Gonzalez-Garcia, M. Maltoni, T. Schwetz, and A. Zhou, “The fate of hints: updated global analysis of three-flavor neutrino oscillations,” *JHEP* **09** (2020) 178, [arXiv:2007.14792 \[hep-ph\]](#).
- [81] F. Capozzi, E. Di Valentino, E. Lisi, A. Marrone, A. Melchiorri, and A. Palazzo, “The unfinished fabric of the three neutrino paradigm,” *Phys.Rev.D* **104** (7, 2021) 083031, [arXiv:2107.00532 \[hep-ph\]](#).
- [82] **LZ** Collaboration, J. Aalbers *et al.*, “A search for new physics in low-energy electron recoils from the first LZ exposure,” [arXiv:2307.15753 \[hep-ex\]](#).

- [83] **XENON** Collaboration, E. Aprile *et al.*, “Excess electronic recoil events in XENON1T,” *Phys. Rev. D* **102** no. 7, (2020) 072004, [arXiv:2006.09721 \[hep-ex\]](#).
- [84] **LZ** Collaboration, J. Aalbers *et al.*, “Background determination for the LUX-ZEPLIN dark matter experiment,” *Phys. Rev. D* **108** no. 1, (2023) 012010, [arXiv:2211.17120 \[hep-ex\]](#).
- [85] P. Ilten, Y. Soreq, M. Williams, and W. Xue, “Serendipity in dark photon searches,” *JHEP* **06** (2018) 004, [arXiv:1801.04847 \[hep-ph\]](#).
- [86] E. M. Riordan *et al.*, “A Search for Short Lived Axions in an Electron Beam Dump Experiment,” *Phys. Rev. Lett.* **59** (1987) 755.
- [87] J. D. Bjorken, S. Ecklund, W. R. Nelson, A. Abashian, C. Church, B. Lu, L. W. Mo, T. A. Nunamaker, and P. Rassmann, “Search for Neutral Metastable Penetrating Particles Produced in the SLAC Beam Dump,” *Phys. Rev. D* **38** (1988) 3375.
- [88] A. Bross, M. Crisler, S. H. Pordes, J. Volk, S. Errede, and J. Wrbanek, “A Search for Shortlived Particles Produced in an Electron Beam Dump,” *Phys. Rev. Lett.* **67** (1991) 2942–2945.
- [89] A. Konaka *et al.*, “Search for Neutral Particles in Electron Beam Dump Experiment,” *Phys. Rev. Lett.* **57** (1986) 659.
- [90] M. Davier and H. Nguyen Ngoc, “An Unambiguous Search for a Light Higgs Boson,” *Phys. Lett. B* **229** (1989) 150–155.
- [91] J. D. Bjorken, R. Essig, P. Schuster, and N. Toro, “New Fixed-Target Experiments to Search for Dark Gauge Forces,” *Phys. Rev. D* **80** (2009) 075018, [arXiv:0906.0580 \[hep-ph\]](#).
- [92] S. Andreas, C. Niebuhr, and A. Ringwald, “New Limits on Hidden Photons from Past Electron Beam Dumps,” *Phys. Rev. D* **86** (2012) 095019, [arXiv:1209.6083 \[hep-ph\]](#).
- [93] J. Blumlein *et al.*, “Limits on neutral light scalar and pseudoscalar particles in a proton beam dump experiment,” *Z. Phys. C* **51** (1991) 341–350.
- [94] J. Blumlein *et al.*, “Limits on the mass of light (pseudo)scalar particles from Bethe-Heitler e^+e^- and $\mu^+\mu^-$ pair production in a proton - iron beam dump experiment,” *Int. J. Mod. Phys. A* **7** (1992) 3835–3850.
- [95] J. Blumlein and J. Brunner, “New Exclusion Limits for Dark Gauge Forces from Beam-Dump Data,” *Phys. Lett. B* **701** (2011) 155–159, [arXiv:1104.2747 \[hep-ex\]](#).
- [96] J. Blümlein and J. Brunner, “New Exclusion Limits on Dark Gauge Forces from Proton Bremsstrahlung in Beam-Dump Data,” *Phys. Lett. B* **731** (2014) 320–326, [arXiv:1311.3870 \[hep-ph\]](#).
- [97] **CHARM** Collaboration, F. Bergsma *et al.*, “Search for Axion Like Particle Production in 400-GeV Proton - Copper Interactions,” *Phys. Lett. B* **157** (1985) 458–462.
- [98] S. N. Gninenko, “Constraints on sub-GeV hidden sector gauge bosons from a search for heavy neutrino decays,” *Phys. Lett. B* **713** (2012) 244–248, [arXiv:1204.3583 \[hep-ph\]](#).
- [99] **NOMAD** Collaboration, P. Astier *et al.*, “Search for heavy neutrinos mixing with tau neutrinos,” *Phys. Lett. B* **506** (2001) 27–38, [arXiv:hep-ex/0101041](#).
- [100] G. Bernardi *et al.*, “Search for Neutrino Decay,” *Phys. Lett. B* **166** (1986) 479–483.
- [101] S. N. Gninenko, “Stringent limits on the $\pi^0 \rightarrow \gamma X$, $X \rightarrow e^+e^-$ decay from neutrino experiments and constraints on new light gauge bosons,” *Phys. Rev. D* **85** (2012) 055027, [arXiv:1112.5438 \[hep-ph\]](#).
- [102] H. Merkel *et al.*, “Search at the Mainz Microtron for Light Massive Gauge Bosons Relevant for the Muon $g-2$ Anomaly,” *Phys. Rev. Lett.* **112** no. 22, (2014) 221802, [arXiv:1404.5502 \[hep-ex\]](#).
- [103] **APEX** Collaboration, S. Abrahamyan *et al.*, “Search for a New Gauge Boson in Electron-Nucleus Fixed-Target Scattering by the APEX Experiment,” *Phys. Rev. Lett.* **107** (2011) 191804, [arXiv:1108.2750 \[hep-ex\]](#).
- [104] **BaBar** Collaboration, J. P. Lees *et al.*, “Search for a Dark Photon in e^+e^- Collisions at BaBar,” *Phys. Rev. Lett.* **113** no. 20, (2014) 201801, [arXiv:1406.2980 \[hep-ex\]](#).
- [105] **KLOE-2** Collaboration, F. Archilli *et al.*, “Search for a vector gauge boson in ϕ meson decays with the KLOE detector,” *Phys. Lett. B* **706** (2012) 251–255, [arXiv:1110.0411 \[hep-ex\]](#).
- [106] **KLOE-2** Collaboration, A. Anastasi *et al.*, “Limit on the production of a new vector boson in $e^+e^- \rightarrow U\gamma$, $U \rightarrow \pi^+\pi^-$ with the KLOE experiment,” *Phys. Lett. B* **757** (2016) 356–361, [arXiv:1603.06086 \[hep-ex\]](#).
- [107] **LHCb** Collaboration, R. Aaij *et al.*, “Search for Dark Photons Produced in 13 TeV pp Collisions,” *Phys. Rev. Lett.* **120** no. 6, (2018) 061801, [arXiv:1710.02867 \[hep-ex\]](#).

- [108] **NA48/2** Collaboration, J. R. Batley *et al.*, “Search for the dark photon in π^0 decays,” *Phys. Lett. B* **746** (2015) 178–185, [arXiv:1504.00607 \[hep-ex\]](#).
- [109] M. Bauer, P. Foldenauer, and J. Jaeckel, “Hunting All the Hidden Photons,” *JHEP* **07** (2018) 094, [arXiv:1803.05466 \[hep-ph\]](#).
- [110] **TEXONO** Collaboration, M. Deniz *et al.*, “Measurement of Nu(e)-bar -Electron Scattering Cross-Section with a CsI(Tl) Scintillating Crystal Array at the Kuo-Sheng Nuclear Power Reactor,” *Phys. Rev. D* **81** (2010) 072001, [arXiv:0911.1597 \[hep-ex\]](#).
- [111] R. Harnik, J. Kopp, and P. A. N. Machado, “Exploring nu Signals in Dark Matter Detectors,” *JCAP* **07** (2012) 026, [arXiv:1202.6073 \[hep-ph\]](#).
- [112] G. Bellini *et al.*, “Precision measurement of the 7Be solar neutrino interaction rate in Borexino,” *Phys. Rev. Lett.* **107** (2011) 141302, [arXiv:1104.1816 \[hep-ex\]](#).
- [113] **CHARM-II** Collaboration, P. Vilain *et al.*, “Measurement of differential cross-sections for muon-neutrino electron scattering,” *Phys. Lett. B* **302** (1993) 351–355.
- [114] **NA64** Collaboration, D. Banerjee *et al.*, “Improved limits on a hypothetical X(16.7) boson and a dark photon decaying into e^+e^- pairs,” *Phys. Rev. D* **101** no. 7, (2020) 071101, [arXiv:1912.11389 \[hep-ex\]](#).
- [115] **NA64** Collaboration, Y. M. Andreev *et al.*, “Search for a New B-L Z’ Gauge Boson with the NA64 Experiment at CERN,” *Phys. Rev. Lett.* **129** no. 16, (2022) 161801, [arXiv:2207.09979 \[hep-ex\]](#).
- [116] **NA64** Collaboration, Y. M. Andreev *et al.*, “Search for Light Dark Matter with NA64 at CERN,” *Phys. Rev. Lett.* **131** no. 16, (2023) 161801, [arXiv:2307.02404 \[hep-ph\]](#).
- [117] Y. M. Andreev *et al.*, “Exploration of the Muon $g - 2$ and Light Dark Matter explanations in NA64 with the CERN SPS high energy muon beam,” [arXiv:2401.01708 \[hep-ex\]](#).
- [118] **BaBar** Collaboration, J. P. Lees *et al.*, “Search for Invisible Decays of a Dark Photon Produced in e^+e^- Collisions at BaBar,” *Phys. Rev. Lett.* **119** no. 13, (2017) 131804, [arXiv:1702.03327 \[hep-ex\]](#).
- [119] T. Aoyama *et al.*, “The anomalous magnetic moment of the muon in the Standard Model,” *Phys. Rept.* **887** (2020) 1–166, [arXiv:2006.04822 \[hep-ph\]](#).
- [120] G.-y. Huang, T. Ohlsson, and S. Zhou, “Observational Constraints on Secret Neutrino Interactions from Big Bang Nucleosynthesis,” *Phys. Rev. D* **97** no. 7, (2018) 075009, [arXiv:1712.04792 \[hep-ph\]](#).
- [121] S.-P. Li and X.-J. Xu, “Production rates of dark photons and Z’ in the Sun and stellar cooling bounds,” *JCAP* **09** (2023) 009, [arXiv:2304.12907 \[hep-ph\]](#).
- [122] J. H. Chang, R. Essig, and S. D. McDermott, “Revisiting Supernova 1987A Constraints on Dark Photons,” *JHEP* **01** (2017) 107, [arXiv:1611.03864 \[hep-ph\]](#).
- [123] D. Croon, G. Elor, R. K. Leane, and S. D. McDermott, “Supernova Muons: New Constraints on Z’ Bosons, Axions and ALPs,” *JHEP* **01** (2021) 107, [arXiv:2006.13942 \[hep-ph\]](#).
- [124] A. Caputo, G. Raffelt, and E. Vitagliano, “Muonic boson limits: Supernova redux,” *Phys. Rev. D* **105** no. 3, (2022) 035022, [arXiv:2109.03244 \[hep-ph\]](#).
- [125] A. Caputo, G. Raffelt, and E. Vitagliano, “Radiative transfer in stars by feebly interacting bosons,” *JCAP* **08** no. 08, (2022) 045, [arXiv:2204.11862 \[astro-ph.SR\]](#).
- [126] G. Alonso-Álvarez, K. Bleau, and J. M. Cline, “Distortion of neutrino oscillations by dark photon dark matter,” *Phys. Rev. D* **107** no. 5, (2023) 055045, [arXiv:2301.04152 \[hep-ph\]](#).
- [127] M. Escudero, D. Hooper, G. Krnjaic, and M. Pierre, “Cosmology with A Very Light $L_\mu - L_\tau$ Gauge Boson,” *JHEP* **03** (2019) 071, [arXiv:1901.02010 \[hep-ph\]](#).
- [128] D. F. G. Fiorillo, G. G. Raffelt, and E. Vitagliano, “Strong Supernova 1987A Constraints on Bosons Decaying to Neutrinos,” *Phys. Rev. Lett.* **131** no. 2, (2023) 021001, [arXiv:2209.11773 \[hep-ph\]](#).
- [129] K. Akita, S. H. Im, M. Masud, and S. Yun, “Limits on heavy neutral leptons, Z’ bosons and majorons from high-energy supernova neutrinos,” [arXiv:2312.13627 \[hep-ph\]](#).